



THE UNIVERSITY *of* EDINBURGH

Edinburgh Research Explorer

The Effects of bead overlap on chromatographic performance in 3D printed packed bed columns

Citation for published version:

Nawada, S, Dimartino, S & Fee, CJ 2014, 'The Effects of bead overlap on chromatographic performance in 3D printed packed bed columns', *International Labmate*.

Link:

[Link to publication record in Edinburgh Research Explorer](#)

Document Version:

Publisher's PDF, also known as Version of record

Published In:

International Labmate

General rights

Copyright for the publications made accessible via the Edinburgh Research Explorer is retained by the author(s) and / or other copyright owners and it is a condition of accessing these publications that users recognise and abide by the legal requirements associated with these rights.

Take down policy

The University of Edinburgh has made every reasonable effort to ensure that Edinburgh Research Explorer content complies with UK legislation. If you believe that the public display of this file breaches copyright please contact openaccess@ed.ac.uk providing details, and we will remove access to the work immediately and investigate your claim.



The Effects of Bead Overlap on Performance of 3D Printed Packed Bed Columns

Suhas Nawada, Simone Dimartino, Conan Fee,
Department of Chemical & Process Engineering and Biomolecular Interaction Centre, University of Canterbury, Private Bag 4800, Christchurch 8041, New Zealand

We propose the use of 3D printing as a production method for chromatography columns with precise control over particle size, shape, orientation and placement. In this paper, we introduce the concept of overlapping beads for structural stability and create columns with differing degrees of bead overlap, leading to different extra-particle porosities. Geometrical analysis and residence time distribution studies have shown that the experimental porosities were consistent with the designed porosity of the columns. This study demonstrates the fine control of packing features that 3D printing can offer in the field of chromatography.

The column preparation process has traditionally involved 'jam-packing' columns to the maximum packing density that is possible with slurry packing. A mathematical limit of packing density $\eta = \frac{\pi}{\sqrt{12}}$, or $\eta = 0.636$ random close packing (RCP), is generally considered to be the upper limit both in terms of packing density and performance in packed bed chromatography. The particle shape, size and orientation are a by-product of the physico-chemical properties of the stationary phase as well as the slurry packing procedure [1, 2]. Because no two randomly packed configurations are identical, predictions of column performance have relied on empirical models, rather than an a-priori consideration of the exact packed bed geometries.

The two major parameters that are used to predict column performance are extra-particle porosity and a shape factor used in the Darcy, Karman, Cozeny and Ergun equations. Extra-particle porosity is often used as a rule of thumb to describe the packed bed homogeneity, tortuosity and, in combination with the particle diameter, internal surface area. Because these four parameters are interdependent in the case of random packing, it has been impossible to isolate any single geometric parameter for further study.

Equations predicting the height equivalent theoretical plates (HETP) require a term for 'packing quality', an all-encompassing term to describe packing heterogeneity, any structural defects in the packing and particle shape and size distributions. The packing quality is determined post-hoc in the form of band broadening. The van Deemter equation, for example, has been found to fit experimental data on plate heights with good accuracy. However, this does not necessarily mean that the effects of packing geometry on HETP are well understood. To quote Gritti et. al. "Despite this good fit, it is generally recognised that the best parameters provided by this mathematical exercise are purely empirical and void of physical sense" [3].

Because of difficulties in controlling the exact positioning of beads in packed beds, efforts to investigate packing geometry have been limited to computational studies, without experimental validation. Simulations used to study random packed columns have traditionally relied on iterative algorithms such as the Jodrey-Tory, Monte Carlo or Lubovchesky-Stillinger algorithms to produce the packing arrangements [4]. While it is possible to achieve the theoretical RCP limits and control several important geometric parameters using these algorithms, it has not been possible to recreate the exact packed bed geometries that the slurry packing process produces. The algorithms assume, for the sake of mathematical simplicity, that the particles are perfectly spherical and identical in shape and size, in contrast to the case in actual chromatography columns, which are known to have beads of varying shapes and a range of particle sizes. While CFD studies have shown the effects of several key packing parameters on band-broadening, a disconnect between the computational and experimental studies has remained.

One approach to avoid the problems faced in random packing would be to produce chromatography columns with an ordered lattice of beads. Apart from achieving optimal packing arrangements and lower extra-particle porosities, this approach would eliminate the band broadening associated with random packing. In addition, traditional empirical models of chromatographic performance would be challenged, because extra-particle porosity does not automatically serve as an indicator of packing quality and tortuosity in the case of ordered packing. For example, it has been shown in computational studies that the traditional three-parameter van Deemter model does not predict plate heights for several ordered packing arrangements [5]. However, while an ordered packing geometry

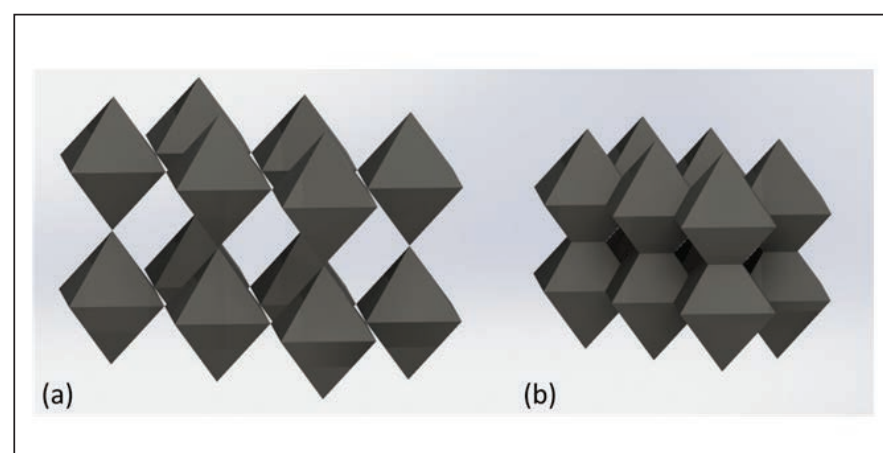


Figure 1. Comparison of non overlapping (a) and overlapping (b) octahedral beads.

has been produced at a capillary scale [6], it has been impossible to produce an ordered arrangement of particles at a scale that is relevant to FPLC systems.

In this study, we used the process of 3D printing, or additive manufacturing, to produce packed beds with control over the placement, size, shape and orientation of each particle [7]. Computer aided design (CAD) models of the entire column, including the packed bed, column walls, fluid distributors and end fittings can be designed and produced as a one-piece system. Using 3D printing, it is possible for the first time to create a perfectly ordered bead arrangement at a large scale. It is also not necessary, as we show in this paper, to limit ourselves to spherical or randomly shaped beads because it is possible to design and create particles of any shape, as long as the resolution of the 3D printer is adequate.

To maintain the structural stability of the packing, a certain amount of overlapping of the beads is necessary. As Figure 1 shows, a packing where only the vertices of the beads are in contact is unlikely to maintain its packing configuration over time. To ensure the packing elements maintain a constant spatial configuration over time, even under mechanical stress, the packing elements need to be securely joined one another by overlaying their vertexes. Such overlap also serves as a tool to gain further insights into the effects of packed bed microstructure on chromatographic performance. In random packing, porosity serves as a reliable predictor of other packing parameters such as tortuosity, internal surface area and packing quality and heterogeneity. In the case of ordered packing, particle shape and packing configuration determine the porosity, the surface area as well as the characteristic shape of the voids through which the mobile phase flows. In addition to shape and orientation, these structural parameters can be appropriately tuned if particle overlap is considered among the design variables to generate the packing morphology.

The goal of the present paper was to assess the quality of 3D printed columns designed with different bead overlaps (Table 1). Porous lattices with varying degrees of bead overlap were first designed and then manufactured by 3D printing. The quality of the printed models was evaluated through optical microscope images, while the flow performance of the columns obtained was tested using residence time distribution experiments.

Table 1. Designed specifications of printed columns

Overlap Factor α	Design porosity ϵ	Design void volume V_{VOID} (ml)	Specific Surface Area S^{-1} (mm $^{-1}$)
1.40	0.575	1.150	9.39
1.45	0.538	1.076	9.97
1.50	0.500	1.000	10.55
1.55	0.463	0.926	11.13

Materials and Methods

CAD Models

As shown in Figure 2a, CAD models comprising a full column including integrated end fittings, fluid distributors and column walls were created in a single stereolithography (STL) file using SolidWorks 2012 (Dassault Systèmes). STL files define the external surfaces of the CAD model as a set of adjacent triangles. It is worth noticing that fewer triangles are necessary to define the external surface of an octahedron than a sphere, hence the computational challenges of producing a full column are dramatically reduced if octahedral elements are chosen instead of spherical beads. For example, a 20.6 ml column containing 10^6 octahedral beads would result in a 1.9 GB CAD file whereas a column containing an identical number of spherical beads would increase the file size by a factor of 252, i.e. around 500 GB, well beyond the processing capabilities of most 3D printing software. This observation is increasingly important for columns having larger volume. For this reason octahedral beads were chosen over the more intuitive spherical beads.

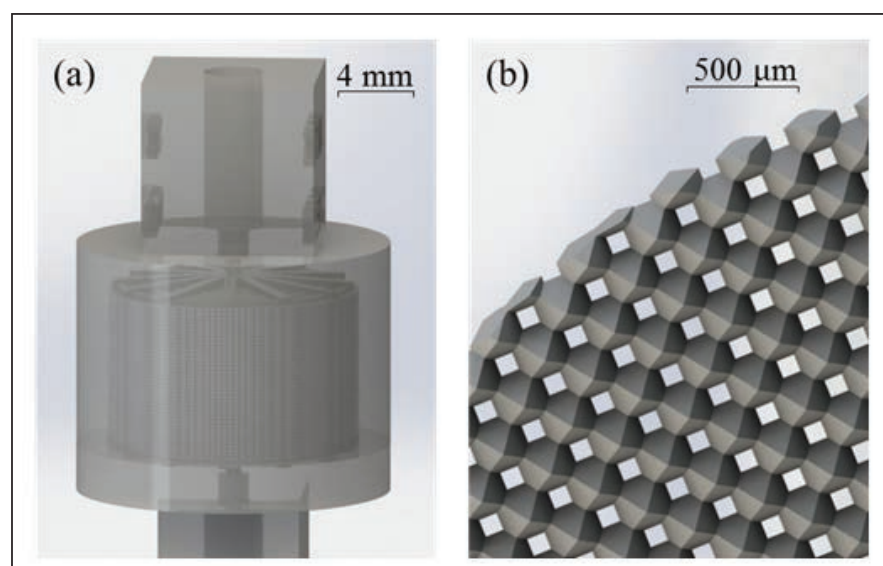


Figure 2. (a) CAD model of chromatography column including end fittings, column walls, flow distributors and column packing. (b) An individual layer in simple cubic packing with a cylindrical cut.

In randomly packed chromatographic beds, the local porosity and local HETP along the column walls are not consistent with the bulk/overall properties of the column, particularly because of the physical constraints posed by the column walls on the arrangement of the packing elements. This problem was eliminated using 3D printing by creating partial beads with the same configuration as the rest of the packing, as seen in Figure 2b. This means that the local porosity along the column walls was identical to that of the bulk packed bed. To measure the degree of overlap between two particles, an overlap factor, α , was introduced as a new geometrical parameter. This is simply defined as the ratio between the actual distance between the centres of two adjacent beads, D_{act} , and the maximum possible distance between their centres if their vertexes are just touching, D_{max}

$$\alpha = \frac{D_{\text{act}}}{D_{\text{max}}} \quad (1)$$

Figure 3 shows the range of porosities that can be obtained by designing lattices characterised by different overlap factors. The overlap factor is a convenient parameter to control, as it directly influences the porosity, while maintaining the same packing configuration, and consequently the same extent of radial and axial dispersion in the bed.

In this study, we compared four columns with overlap factors of $\alpha = 1.40, 1.45, 1.50$ and 1.55 (Table 1). The designed porosity for these packing is in the order of 0.6, namely the range of porosities usually found in randomly packed columns. The printed columns had an internal diameter and a wall thickness of 16 and 2 mm, respectively, and radial flow distributors and collectors were integrated at the inlets and outlets of the printed columns. The total column volume was kept constant at 2 ml (corresponding to a column height of 9.95 mm), meaning that void volume of each column varied with α .

Column Production and Post-Processing

The four columns were printed on a 3DS Projet HD 3500 printer (3D Systems, Rock Hill, SC, USA). In addition to the four whole columns, equivalent 'cutaway' pieces containing packings with the four tested overlap factors were printed for geometrical analysis. To support the overhanging features in the columns, paraffin wax is used as a support material during the printing process. The supporting wax was removed using an alternating series of cyclohexane and water baths at 70°C.

The nominal resolution of the 3D printer is 29 μm , however both the surface finish and positional accuracy of the 3D printer are dependent on several parameters, such as printing material, local temperature and relative humidity. A bead apothem of approximately 115

μm was found to be the lowest octahedron size that the printer could reliably create using a commercial acrylonitrile butadiene styrene (ABS) printing material (Visijet® X, 3D Systems, Rock Hill, SC, USA). The printed columns thus contained beads with apothems of 115 μm . A minimum overlap factor of $\alpha = 1.40$ was chosen because it was determined in initial experiments that this was the minimum required to ensure structural robustness in the packing structure (data not shown).

Residence Time Distribution Tests

To assess the flow properties of the printed columns, an ÄKTA Explorer10™ FPLC system equipped with an auto-sampler (GE Healthcare, Uppsala, Sweden) was used. Residence time distribution (RTD) tests were conducted by first equilibrating the 3D printed columns with 10 column volumes (CVs) of pure water, followed by a 30 μl injection of 1 M NaCl. The concentration profile was measured by monitoring the conductivity signal of the outlet stream. All tests were performed at a flow rate of 10 ml/min, corresponding to a superficial velocity of 298 cm.hr $^{-1}$. The mean residence volume, μ_1 , the variance, σ^2 , and the skewness, γ_1 , of the RTD profiles were calculated using the moment method:

where κ is the conductivity measurement and v is flow volume. The dimensionless residence volume, θ_r^{exp} , was calculated as follows:

$$\mu_1 = \frac{\int_0^\infty \kappa v dv}{\int_0^\infty \kappa dv} \quad (2) \quad \sigma^2 = \frac{\int_0^\infty \kappa (v - \mu_1)^2 dv}{\int_0^\infty \kappa dv} \quad (3) \quad \gamma_1 = \frac{\int_0^\infty \kappa (v - \mu_1)^3 dv}{\sigma^3 \int_0^\infty \kappa dv} \quad (4)$$

$$\theta_r^{\text{exp}} = \frac{\mu_1}{V_{\text{VOID}}} \quad (5)$$

where V_{VOID} is the designed void volume. Other volumes in the system were less than 4% so their contribution to the first moment (μ_1) was neglected. θ_r^{exp} is an indicator of the quality of the printed chromatography columns. In fact, a dimensionless residence time close to unity indicates both good control over particle shape at the printer's limiting resolution, and good positional accuracy of the 3D packing elements in the lattice. θ_r^{exp} is extremely valuable to assess the printing quality of packed bed columns, and is sensitive to subtle changes in the key geometrical parameters, including the overlap factor. For example, the differences in porosity across the four columns studied in the present work were relatively small, with a 7.5% change in porosity for each 0.05 increment in α . Even small errors in printing of the beads would make the four columns indistinguishable in their flow characteristics and chromatographic performance.

Results and Discussion

Geometrical Analysis

Figure 4 shows optical microscope images of the octahedral packings manufactured with different overlap factors. It is apparent that the beads are largely octahedral in shape and that the packing arrangements are highly ordered, similar to a range of packings we reported previously [7]. It is worth noting that features such as build size, orientation and materials could potentially result in imperfections in the printed part (as seen in the lower right hand side of Figure 4c, for example). Fine control of the lattice shape was confirmed through geometrical analysis of the microscope images, as summarised in Table 2. The results from the geometrical analysis of these cutaway samples are consistent with design specifications of both bead and pore sizes, with a mean error of 2.4%, showing that 3D printing can create columns with only subtle differences in column packing parameters. It can reasonably be assumed that the whole columns printed would display similarly good fidelity with the CAD models.

Residence Time Distribution Profiles

Normalised residence time distribution curves of two printed columns are shown in Figure 5, where κ represents the normalised conductivity readings (i.e. conductivity data normalised to obtain a unit area under the curve). The peak maxima of the curves depend on the degree of overlap, consistent with expected extra-particle porosity. Figure 6 shows the comparison between theoretical (designed) and experimental residence times for the four columns tested, while Table 3 summarises the results obtained from the moment analysis.

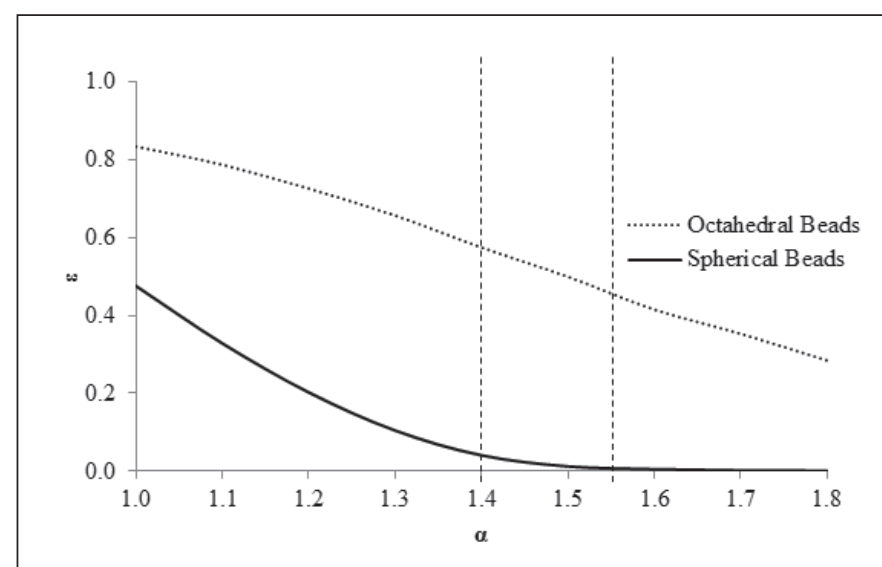


Figure 3. The effects of bead overlap on extra particle porosity in a simple cubic packing configuration. The vertical bars identify the range of overlap factors investigated in the present study.

Table 2. Geometric characteristics of bead packing in cutaway sample pieces

Overlap	Porosity		Pore Flat to Flat Distance (μm)	
	Designed	Geometrical analysis	Designed	Geometrical analysis
1.40	0.575	0.561 ± 0.033	121.3	118.3 ± 6.8
1.45	0.538	0.542 ± 0.008	107.3	108.1 ± 6.2
1.50	0.501	0.511 ± 0.051	94.3	96.2 ± 5.5
1.55	0.463	0.442 ± 0.027	82.2	78.5 ± 4.5

The number of pores analyzed were $n = 63, 64, 71$ and 80 for $\alpha = 1.40, 1.45, 1.50$ and 1.55 , respectively. The errors given are $\epsilon_i = 2\sigma$ where σ is the standard deviation.

Table 3. Performance characteristics of the four tested columns

α	μ_1 (ml)	θ_r^{exp}	γ_1
1.40	1.278	1.11	0.407
1.45	1.078	1.00	0.617
1.50	0.991	0.99	0.935
1.55	0.917	0.99	1.134

The values in Table 3 highlight the extremely good agreement between the design and experimental void volumes in all but one column ($\alpha = 1.40$). It can also be seen that there is a linear relationship between the overlap factors and peak skewness. It is generally thought that a lower porosity and greater internal surface area would result in a more symmetrical RTD profile and greater chromatographic resolution [8]. In this instance, the designed specific surface areas of the $\alpha = 1.40$ and $\alpha = 1.55$ columns were 9.39 and 11.13 mm^{-1} , respectively, while the skewness values for the latter column was significantly higher. A possible reason for this unexpected result could involve the printer resolution, where micro-rugosities on the bead surface are produced during the printing process – see Figure 4. In a column with greater bead overlap, and therefore smaller pores, the rugosity could have greater consequences in terms of band broadening. This finding suggests that extra-particle porosity alone is not a significant parameter in column performance but other factors as small imperfections in the outer shape of the beads will also influence column behaviour. Efforts to improve the chromatographic performance of 3D printed columns must therefore focus on ensuring homogenous flow channels instead of achieving the lowest porosity that the 3D printing process would allow.

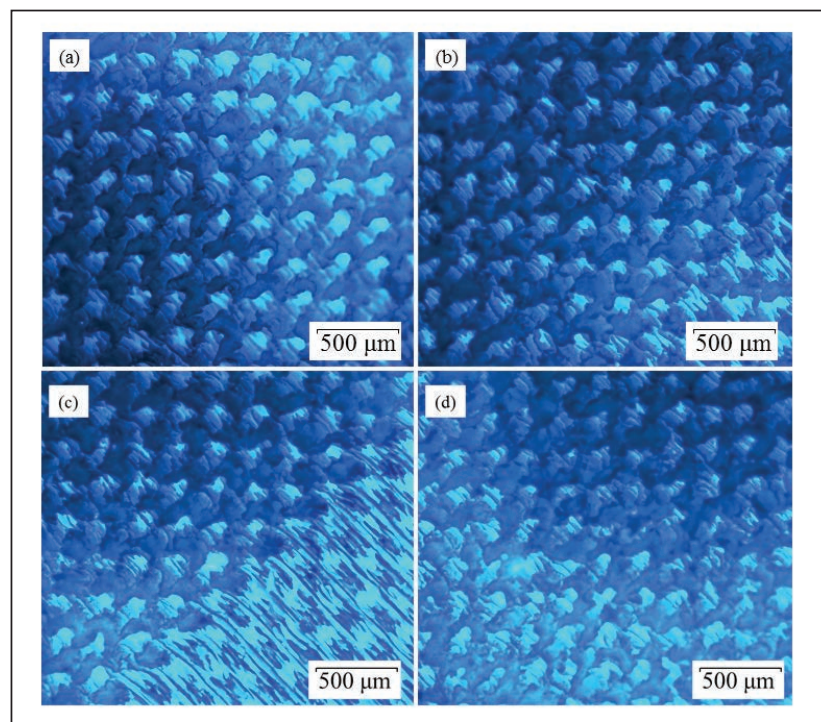


Figure 4. Microscope images of cutaway sample parts displaying samples with; (a) $\alpha = 1.40$, (b) $\alpha = 1.45$, (c) $\alpha = 1.50$, (d) $\alpha = 1.55$ at a magnification of $5\times$.

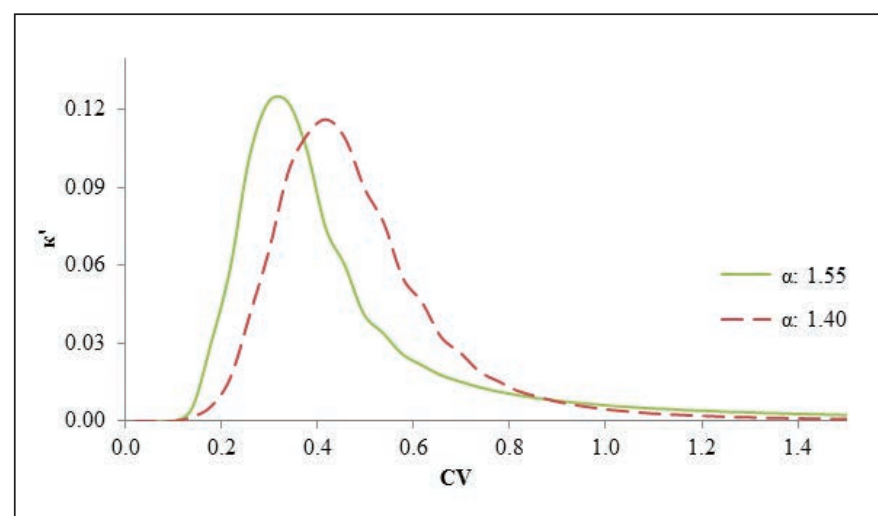


Figure 5. Typical residence time distribution profiles of two columns.

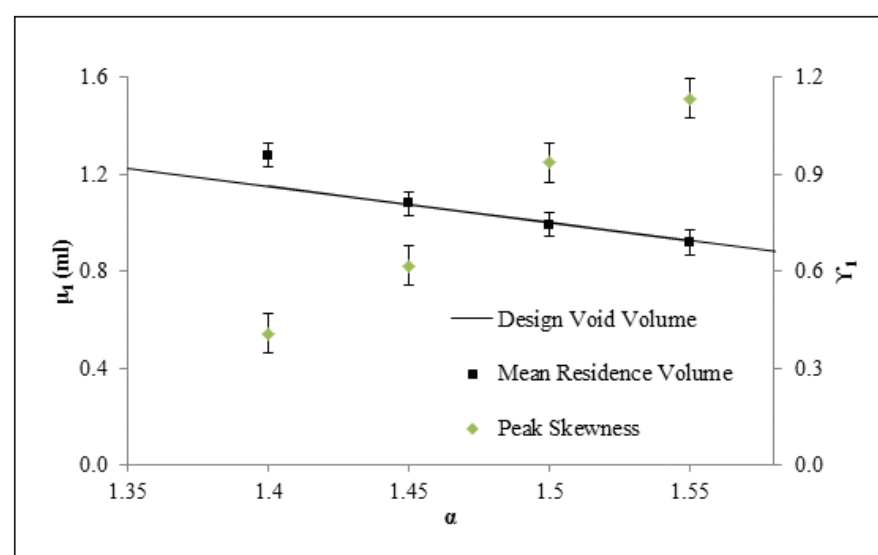


Figure 6. Comparison of theoretical and experimentally determined void volumes and peak skewness of RTD profiles.

Conclusions

We have demonstrated the ability of 3D printing to create whole columns containing an ordered lattice of beads, with only subtle changes in column packing parameters, requiring fine control of bead positioning and overlap. The experimentally determined mean residence volumes were consistent with the design void volumes, indicating a good agreement between the CAD models and 3D printed artefacts.

Contrary to conventional wisdom, our findings have shown that a low extra-particle porosity and a high internal surface area do not automatically imply more symmetrical RTD profiles, for the case of 3D printed, ordered packings.

Due to the precision, scale and versatility that 3D printing offers in the production of chromatography columns, we expect this approach to revolutionise the field of packed bed research, enabling greater insights into the effects of morphological features of packed beds on performance.

References

- [1] Vissers J.P.C., Hoebein M.A., Laven J., Claessens H.A., Cramers C.A., Hydrodynamic aspects of slurry packing processes in microcolumn liquid chromatography. *Journal of Chromatography A*, 2000, 883: p. 11-25.
- [2] Zimina T., Smith R.M., Highfield J.C., Myers P., King B.W., Study of the flow development during the slurry packing of microcolumns for liquid chromatography. *Journal of Chromatography A*, 1996, 728: p. 33-45.
- [3] Gritti F., Guiochon G., Mass transfer kinetics, band broadening and column efficiency. *Journal of Chromatography A*, 2012, 1221: p. 2-40.
- [4] Baranau V., Hlushkow D., Khirevich S., Tallarek U., Pore-size entropy of random hard-sphere packings. *RSC Publishing - Soft Matter*, 2013, 9: p. 3361-3372.
- [5] Schure M.R., Kroll D.M., Davis H.T., Simulation of ordered packed beds in chromatography. *Journal of Chromatography A*, 2004, 1031: p. 79-86.
- [6] Malkin D.S., Wei B., Foigel A.J., Staats S. L., Wirth M.J., Submicrometer plate heights for capillaries packed with silica colloidal crystals. *Analytical Chemistry*, 2010, 82: p. 2175-2177.
- [7] Fee C.J., Nawada S., Dimartino S., 3D printed porous media columns with fine control of column packing morphology. *Journal of Chromatography A*, 2014, 1333: p.18-24.
- [8] Guiochon G., Felinger A., Shirazi D.G., *Fundamentals of Preparative and Nonlinear Chromatography*, 2nd ed. 2006, Amsterdam: Elsevier.



Read, Share and Comment on this Article, visit: www.labmate-online.com/articles